Journal Pre-proofs

Systematic screening of photopolymer resins for Stereolithography (SLA) 3D printing of solid oral dosage forms: investigation of formulation factors on printability outcomes

Carlo Curti, Daniel J. Kirby, Craig A. Russell

Please cite this article as: C. Curti, D.J. Kirby, C.A. Russell, Systematic screening of photopolymer resins for Stereolithography (SLA) 3D printing of solid oral dosage forms: investigation of formulation factors on printability outcomes, *International Journal of Pharmaceutics* (2024), doi: https://doi.org/10.1016/j.ijpharm. 2024.123862

This is a PDF file of an article that has undergone enhancements after acceptance, such as the addition of a cover page and metadata, and formatting for readability, but it is not yet the definitive version of record. This version will undergo additional copyediting, typesetting and review before it is published in its final form, but we are providing this version to give early visibility of the article. Please note that, during the production process, errors may be discovered which could affect the content, and all legal disclaimers that apply to the journal pertain.

Systematic screening of photopolymer resins for Stereolithography (SLA) 3D printing of solid oral dosage forms: investigation of formulation factors on printability outcomes.

Carlo Curti [a], Daniel J. Kirby [a], Craig A. Russell [a, *]

[a] School of Pharmacy, Aston University, Aston Triangle, Birmingham B4 7ET, UK

[*] Correspondence to: c.russell6@aston.ac.uk; tel: +4401212043077

Highlights

- Reducing the amount of TPO as low as 0.05% w/w leads to better printability outcomes with the further advantage of reduced costs and lower dose-related toxicity concerns.
- The inclusion of high amounts of liquid fillers in photopolymer formulations for SLA 3D printing of medicines should take into account a likely decrease in printing quality of the final dosage form.
- Glycerol cannot be used as a liquid filler for PEGDA-based photopolymer resins for SLA 3D printing due to its immiscibility with the photopolymer.

Abstract

Pharmaceutical three-dimensional printing (3DP) is now in its golden age. Recent years have seen a dramatic increase in the research in 3D printed pharmaceuticals due to their potential to deliver highly personalised medicines, thus revolutionising the way medicines are designed, manufactured, and dispensed. A particularly attractive 3DP technology used to manufacture medicines is stereolithography (SLA), which features key advantages in terms of printing resolution and compatibility with thermolabile drugs. Nevertheless, the enthusiasm for pharmaceutical SLA has not been followed by the introduction of novel excipients specifically designed for the fabrication of medicines; hence, the choice of biocompatible polymers and photoinitiators available is limited. This work provides an insight on how to maximise the usefulness of the limited materials available by evaluating how different formulation factors affect printability outcomes of SLA 3D printed medicines. 156 photopolymer formulations were systematically screened to evaluate the influence of factors including photoinitiator amount, photopolymer molecular size, and type and amount of liquid filler on the printability outcomes. Collectively, these factors were found highly influential in modulating the print quality of the final dosage forms. Findings provide enhanced understanding of formulation parameters informing the future of SLA 3D printed medicines and the personalised medicines revolution.

Key Words: 3D printing; stereolithography; solid oral dosage forms; formulation development; personalised medicine

1. Introduction

Since the first Food and Drug Administration (FDA) approval of a 3D printed drug product in 2015, research in the field of pharmaceutical 3D printing has grown exponentially due to the paradigm shift announced alongside the introduction and rapid development of such technology (Curti, Kirby and Russell, 2020; Muhindo et al., 2023). 3D printers have, therefore, been proposed as flexible manufacturing platforms, making it possible to produce medicines on demand, in a variety of settings including hospital pharmacies, natural disasters, remote areas, and even in space, starting a new era in pharmaceutical compounding (Dooms and Carvalho, 2018; Goyanes et al., 2019; Seoane-Viaño et al., 2021; Seoane-Viaño et al., 2022). Indeed, as opposed to conventional manufacturing methods designed for mass production of solid oral dosage forms, 3D printers have the potential for a wide number of applications, such as the fabrication of immediate or controlled release dosage forms (Khaled et al., 2018; Pietrzak et al., 2015), osmotic or floating tablets (Khaled et al., 2015; Li et al., 2018), and even gummies or chocolate formulations specifically designed for paediatric use (Karavasili et al., 2020; Tagami et al., 2021). Furthermore, 3D printed solid oral dosage forms can be easily tailored to the needs of individual patients, thus revolutionising the way medicines are designed, manufactured, and dispensed (Konta et al., 2017).

Currently, extrusion based 3D printing technologies, such as fused deposition modelling (FDM), account for most of the applications of 3D printing for the making of pharmaceuticals, mainly due to the key advantage of being able to use conventional excipients approved for pharmaceutical use as feedstock material; still, several 3DP technologies have been so far investigated for this purpose (Serrano et al., 2023). One attractive technique is stereolithography (SLA), a subtype of vat-photopolymerisation 3D printing, which has been investigated in several studies for its advantages over other techniques (Curti et al., 2021; Martinez et al., 2017; Robles Martinez et al., 2019; Wang et al., 2016; Xu et al., 2021, 2020). Indeed, SLA features an unequalled printing resolution, is compatible with thermolabile drugs, and does not use powders as feedstock material, thus avoiding flowability issues (Xu et al., 2021). Still, the pharmaceutical application of SLA remains limited. One major reason for this is the very limited number of biocompatible photoinitiators and photopolymers available, with none of these listed as generally recognised as safe (GRAS) (Pan et al., 2023). Furthermore, the raw materials needed to assemble photopolymerisable resins for SLA are relatively expensive, and formulations are generally required to be produced in large bulks, discouraging extensive formulation development work aimed to investigate the printability of novel photopolymers (Curti et al., 2021).

While novel excipients specifically designed for SLA 3D printing of solid oral dosage forms should be implemented (Xu et al., 2021), it is important to acquire deep knowledge of the materials currently available, to maximise their usefulness and to avoid undesired reactions (Xu et al., 2020). Specifically, it should be investigated how the use of specific types and amounts of the photopolymer components affect the printing quality of the final product, with the aim to drive future formulation design work and even machine learning tools (Elbadawi et al., 2020).

Therefore, in this work the influence of several formulation factors on the printability outcomes of 156 drug-free photopolymer formulations was investigated. Prior to this, a preliminary screening aimed to identify the most suitable photoinitiators for SLA 3D printing was performed. Results generated in this work can contribute to the future implementation of SLA 3D printing in pharmaceutics, where flexible, multipurpose and drug-loadable photopolymer resins will be needed to fabricate on demand quality pharmaceuticals.

2. Material and methods

2.1 Chemicals

Polyethylene glycol diacrylate (PEGDA) with molecular number (Mn) 250, 575, and 700, N-vinyl-pyrrolidone (N-VP), polyethylene glycol 300 (PEG300), propylene glycol (PG), glycerol and the photoinitiators diphenyl (2,4,6-trimethylbenzoyl) phosphine oxide (TPO), 2-hydroxy-2-methylpropiophenone (HMPP), 2-hydroxy-4-(2-hydroxy ethoxy)-2-methyl propiophenone (HHEMPP),

Commented [CC1]: Reference implemented with up to date literature.

Commented [CC2]: Self citation changed with up to date reference.

Commented [CC3]: Self citation changed with up to date reference.

riboflavin (RF), and triethanolamine were purchased from Sigma-Aldrich, UK. Acetophenone (ACP) and camphorquinone (CQ) were purchased from Alfa Aesar, UK.

2.2 UV-visible spectrophotometry

The wavelength of maximum absorption (λ max) of each photoinitiator (PI) was determined through UV-Vis spectrophotometry carried out on a Genesys 10S UV/Vis Spectrophotometer (Thermo Fisher Scientific, USA). A 50% v/v water/methanol solution was used to dissolve each PI. Prior to analysis, a baseline was acquired by running a blank sample. PI samples were scanned within a range of 190 to 500 nm with an interval of 1 nm.

2.3 Formulation of photopolymer resins

All photopolymer resin formulations described in this paper were prepared following the same procedure described in our previous work (Curti et al., 2021). Firstly, PEGDA was directly weighed in 30 mL glass vials. Solid PI were weighed separately and later transferred to the photopolymer base, while liquid PI were accurately withdrawn and directly transferred to the PEGDA vials. Then, any other liquid component was added to the PEGDA vials, and the mixtures were stirred for 12 hours at room temperature until complete solubilisation of the PI. All operations were carried out away from light by working in dark environment and covering the glass vials with aluminium foil, to avoid premature photopolymerisation of the mixture. Once ready, photopolymer formulations were transferred for 3D printing to a modified SLA apparatus, described in our previous work (Curti et al., 2021).

2.4 Stereolithography 3D printing

PI efficacy and printability of photopolymer resin formulations were evaluated by 3DP test tablets using a modified Form 2 SLA 3D printer (Formlabs Inc., USA). Tablet computer-aided design (CAD) models used in this paper were based on cylindrical tablet designs (12 × 4 mm, diameter × thickness), and were 3D printed directly on the build platform (BP), thus avoiding the use of printing supports. Formulations related to PI efficacy screening were 3D printed setting layer thickness (printing resolution) to 100 μm, while the subsequent printability screening of photopolymer resins was carried out setting layer thickness (printing resolution) to 25 μm, 50 μm, and 100 μm. All formulations were 3D printed in triplicates. At the completion of the 3D printing process, tablet samples were removed from the BP and the uncured resin was removed using filter paper.

2.5 Printability evaluation

To evaluate printability outcomes, we implemented an improved version of a points-based scale previously developed (figure 1) (Curti et al., 2021). In short, a printability score (PS) from 1 to 6 was assigned to each formulation based on the visual observation after a print was completed.

Observation	Formulation remains liquid	Gel-like texture	Polymerised fragments	Incomplete or fallen object	Accurately printed object	Broadening	Defined edges
Printability Score	1	2	3	4	5	6	*
Comments	No polymerisation	Insufficient crosslinking	Partial crosslinking	Failed Print	Successful Print	Uncontrolled polymerisation	Geometrical accuracy
Exemplary Representation							

Figure 1. Points-based printability scale developed to evaluate printability outcomes of SLA 3D printed tablets based on visual observation. For each Printability Score (PS) in the scale, comments and an exemplary representation are reported.

Photopolymer formulations remaining entirely liquid in the resin tank after 3DP were assigned a PS = 1, indicating that no photopolymerisation occurred. Formulations changing to a soft gel-like consistency were given a PS = 2, suggesting that photocrosslinking was too low to form solid structures, while a PS = 3 was used to classify formulations reaching partial crosslinking, as shown by the presence of polymerised debris in the resin tank at the end of the print run. A PS = 4 was used to identify a failed print, in form of a partially or inaccurately 3D printed object, or resulting from the detachment from the BP. A PS = 5 was assigned to fully printed tablets matching the 3D model designed; an extra mark, indicated as *, was assigned to printed tablets showing defined edges indicating high geometrical accuracy of the 3D printed design. As such, a PS = 5* was used to identify the best printability outcome. Photopolymer formulations showing uncontrolled and extensive polymerisation during 3DP, a multiple causes phenomenon significantly compromising the geometrical accuracy of the design, were given a PS = 6.

Ultimately, the inclusion criteria to determine which formulations to consider for the subsequent analysis of formulation factors on printability outcomes were the following:

1) 3D printed tablets presenting a PS = 5*,

2) 3D printed tablets presenting a PS = 5,

3) 3D printed tablets presenting a PS = *,

3. Results and discussion

3.1 Selection of photoinitiators for pharmaceutical SLA 3D printing

Six photoinitiator systems were shortlisted for a preliminary screening aimed to evaluate their suitability for SLA 3D printing of medicines. PI were selected based on the respective safety profiling and previously described use in solid oral dosage forms and/or other biocompatible applications reported in the scientific literature (Bertolotti et al., 1999; Fouassier et al., 2003; Williams et al., 2005; Kochhar et al., 2012; Kamoun et al., 2016; Wang et al., 2016; Martinez et al., 2017; Robles Martinez et al., 2018; Voet et al., 2018; Pan et al., 2019; Chiulan et al., 2021; Chen et al., 2023; Jeencham et al., 2023; Li et al., 2023; Pariskar et al., 2023). A spectrophotometric analysis was carried out on each PI to measure the respective λ max (table 1) and to verify if any of the selected PI absorbed light at the same wavelength of common model drugs meeting the rationale for 3D printing such as paracetamol and theophylline (Curti et al., 2020; Trenfield et al., 2023; Wang et al., 2016). Indeed, considering a λ max of 243 nm for paracetamol (Sirajuddin et al., 2007) and 273 nm for theophylline (Patel et al., 2013), it is evident that HMPP and HHEMPP share the same λ max, respectively. Although evaluating the printability of such model compounds was beyond the scope of this paper, it's worth noting that 3D printing a resin formulation combining paracetamol and HMPP or theophylline and HHEMPP, would likely have an impact on the photopolymerisation process due to the UV absorber capacity of the mentioned drugs (Bail et al., 2016; Gong et al., 2017).

Commented [CC4]: Implemented with up to date references

Table 1. Measured λ max values of the photoinitiators selected for efficacy screening.

Photoinitiator	Abbreviation used	λ max
Diphenyl-(2,4,6-trimethyl benzoyl)-phosphine oxide	TPO	380.5 nm
2-Hydroxy-2-methyl propiophenone	HMPP	243.5 nm

2-Hydroxy-4-(2-hydroxyethoxy)-2-methylpropiophenone	HHEMPP	273.5 nm
Acetophenone	ACP	239.5 nm
Camphorquinone	CQ	468.0 nm
Riboflavin	RF	463.0 nm

3.2 Printability efficacy of photoinitiators for pharmaceutical SLA 3D printing

PI efficacy was evaluated by preparing and 3D printing 12 photopolymer resin formulations, whose composition is described in table 2. Following 3D printing, each PI formulation was assigned a printability score (also reported in table 2) based on the printability scale shown in figure 1.

Table 2. % w/w composition of 12 photopolymer resin formulations designed to evaluate the efficacy of 6 photoinitiator systems . The printability score assigned to each formulation after 3D printing is also reported in the table.

Formulation	PEGDA 700	TPO	HMPP	HHEMPP	ACP	CQ	RF	PS
PIsF1	99.9	0.1	-	-	-	-	-	5*
PIsF2	99.9	-	0.1	-	-	-	-	1
PIsF3	99.9	-	-	0.1	-	-	-	1
PIsF4	99.9	-	-	-	0.1	-	-	1
PIsF5	99.9	-	-	-	-	0.1	-	3
PIsF6	99.9	-	-	-	-	-	0.1	1
PIsF7	99.0	1.0	-	-	-	-	-	6
PIsF8	99.0	-	1.0	-	-	-	-	1
PIsF9	99.0	-	-	1.0	-	-	-	1
PIsF10	99.0	-	-	-	1.0	-	-	1
PIsF11	99.0	-	-	-	-	1.0	-	4

PIsF12	99.0	-	-	-	-	-	1.0	3

Formulation PIsF1, containing 0.1% w/w TPO (TPO), was assigned a PS = 5* indicating its efficacy to 3D print tablets in a well-defined shape (figure 2A). Interestingly, increasing TPO concentration to 1% w/w (formulation PIsF7) caused a high degree of broadening (PS = 6), a phenomenon resulting in a 3D printed tablet whose bottom side had undergone uncontrolled polymerisation (figure 2B). It is worth noting that the use of 1% w/w TPO was already reported in the fabrication of SLA 3D printed dosage forms, with no reports of broadening (Wang et al., 2016). Factors including high extinction coefficients at the irradiation wavelength (resulting in n–π* excitation), high dissociation quantum yields, and excellent reactivity of the primary radicals towards the monomer, suggest that the reactivity of TPO is particularly high (Eibel et al., 2018), and an increase of its concentration will result in high radical generation and polymerisation rate (Meereis et al., 2014), potentially leading to the loss of geometrical control during photopolymerisation. A further explanation could be attributed to the scattering of the light emitted by the laser beam. In fact, when the incident light is scattered, more radiation is delivered to the sideways directions, thus increasing the cure width (C_w), eventually resulting in a reduced printing accuracy (Zakeri et al., 2020).

Formulations containing HMPP, HHEMPP, and ACP, in concentrations of both 0.1% and 1% w/w, were given a PS = 1 because no changes were observed in the photopolymer resin at the end of the print, indicating their inefficacy in initiating photopolymerisation. Based on the spectrophotometric analysis previously carried out on the PI, the observed results were expected as their λ max was found to be in a range of 239.5 nm to 273.5 nm, while the laser in the SLA apparatus emits light radiation with a wavelength of 405 nm. However, other research has proven that these PI hold potential to be successfully used in SLA (Chen et al., 2022; Konasch et al., 2018; Lakkala et al., 2023), and it should be even noted that more recent VAT technologies such as dual-wavelenght digital light processing (DLP) 3D printing could broaden the selection of effective PI (Cazin et al., 2022; Rossegger et al., 2023b, 2023a; Van Der Linden et al., 2020).

Formulations containing CQ at concentrations of 0.1% and 1% w/w were respectively assigned a PS of 3 and 4. Since a PS = 4 indicates a failed print featuring inaccurate or missing details of the 3D printed tablet (figure 2C), CQ will not be further investigated at this stage, although it could be considered for future studies due to its good biocompatibility (Kamoun et al., 2016; Nan et al., 2022; Zanon et al., 2021).

RF was not found to initiate polymerisation when used at 0.1% w/w (PS = 1), while its increase to 1% w/w allowed the formation of partially crosslinked structures (PS = 3) (figure 2D). Surprisingly, these results are in contrast with those found by Martinez (Martinez et al., 2017). However, it should be considered that in this work RF was not solubilised in water to eventually formulate hydrogels, but rather it was mixed with pure PEGDA 700 where it was seen to be slightly soluble.
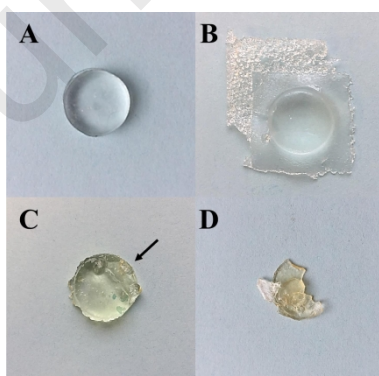
Figure 2. 3D printed tablets produced from (A) 0.1% TPO, (B) 1.0% TPO, (C) 0.1% CQ, and (D) 1.0% RF. The arrow indicates a partially printed edge.

3.3 Formulation of photopolymer resins for SLA 3D printing

Of the six PI analysed through spectrophotometry, TPO showed maximum absorption at 380.5 nm, making it the PI most closely matching the target wavelength of 405 nm emitted by the modified Form 2 3D printer laser. Furthermore, in a preliminary printability screening, TPO allowed for the successful fabrication of non-drug loaded test tablets. As such, TPO emerged as the frontrunner photoinitiator for SLA 3D printing of PEGDA based photopolymer formulations using a 405 nm light source. The next step consisted in the preparation of 156 TPO-based photopolymer resins formulations, according to the formulas already described in our previous work and reported in table A.1. Printability of each formulation was evaluated using the same printability scale described in figure 1. In short, the whole set of photopolymer formulations screened was classified in four groups (figure 3; table A.1).

Out of the 156 formulations tested, 96 did not meet any of the three inclusion criteria described in section 2.5, indicating poor printability outcomes (figure 3, group A).

The remaining 60 formulations met at least one inclusion criterion thus making up a pool labelled as printable formulations (PF, n = 60) (figure 3, group B). Then, formulations in group B meeting inclusion criterion 1 (3D printed tablets presenting a PS = 5*) were subclassified into groups B1 (n = 35; formulations reaching PS = 5* at least for one printing resolution used between 25, 50 or 100 μm) and B2 (n = 5; formulations reaching PS = 5* at each printing resolution used between 25, 50 and 100 μm). Formulations belonging to groups B1 and B2 were jointly labelled as best formulations (BF, n = 40) because a PS = 5* was used to identify the best printability outcome.

The remaining 20 formulations in group B were still considered for the subsequent analysis of printability outcomes because they met inclusion criteria 2 or 3 hence being considered among the Printable Formulations.
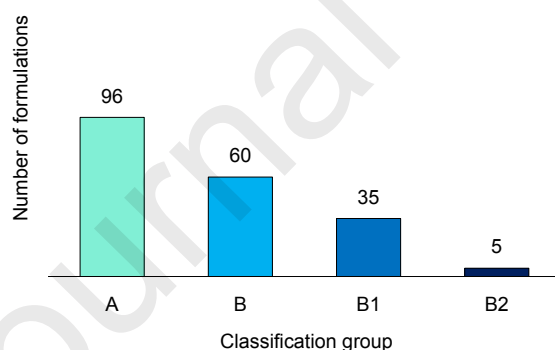

Figure 3. Group classification of photopolymer formulations screened.

3.4 Influence of formulations factors on printability outcomes

3.4.1 Polyethylene glycol diacrylate

The role of PEGDA Mn on printability outcomes was investigated. The graph in figure 4 displays the number of PF and BF containing PEGDA 250, 575, and 700, respectively.

According to the results, PEGDA 250 was the most frequently effective polymer both among PF (26) and BF (19). PEGDA 575 was present in 24 PF and 13 BF, while PEGDA 700 in 10 PF and 8 BF. However, PEGDA 700 showed the highest BF/PF ratio (0.80) in comparison to PEGDA 250 (0.73) and PEGDA 575 (0.54), suggesting that its use is more likely to provide 3D printed tablets in an accurate size and shape. As a result, we indicate PEGDA 700 as the most recommended photocrosslinkable polymer to be considered for the formulation of drug loaded photopolymer resins for SLA 3D printing of medicines with the greatest accuracy.
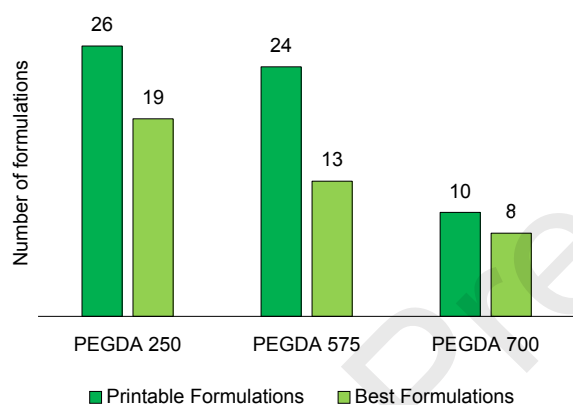
Figure 4. Number of formulations containing PEGDA 250, 575, and 700 classified as printable formulations (PF) and best formulations (BF).

3.4.2 Polyethylene glycol, propylene glycol and glycerol

PEG 300, PG, and glycerol were individually used as liquid fillers combined in different concentrations with PEGDA. Liquid fillers can act as co-solvents to enhance drug solubility in the liquid photopolymer or as release-tuning agents, and their incorporation into SLA printable formulations represents a standard strategy to overcome such issues (Krkobabić et al., 2019; Wang et al., 2016).

The data in figures 5-6 show the number of formulations containing PEG 300 or PG in different concentrations, that were classified as PF and BF.
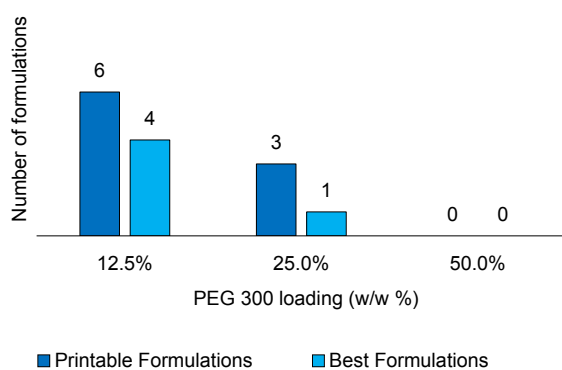
Figure 5. Number of formulations containing PEG 300 classified as printable formulations (PF) and best formulations (BF).

When PEG 300 was used in a concentration of 12.5% w/w, a total of 6 PF and 4 BFs were obtained (figure 5). Doubling PEG 300 concentration to 25% w/w led to the classification of 3 PF and 1 BF, while a further PEG 300 increase to 50% w/w did not allow identification of any PF and BF. Therefore, we can assume that the inclusion of PEG 300 in a concentration of 12.5% w/w was most effective in ensuring good printability, as also indicated by the high BF/PF ratio (0.67). However, previous research (Krkobabić et al., 2019; Wang et al., 2016) has shown that increasing the PEG concentration in the photopolymerisable resin generally leads to an increased drug release from 3D printed dosage forms; as such, this should be considered at the formulation design and development stage.
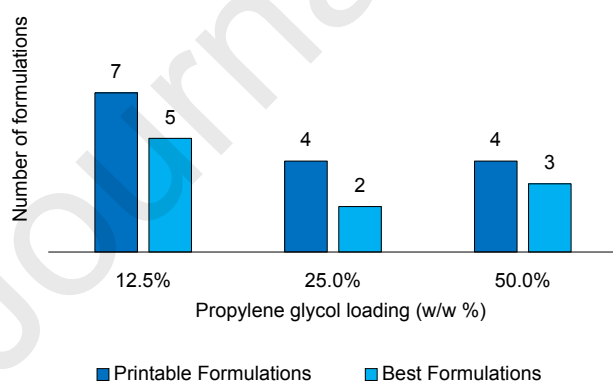

Figure 6. Number of formulations containing propylene glycol classified as printable formulations (PF) and best formulations (BF).

PG provided better results when loaded at higher concentrations, in comparison to PEG 300 (figure 5). Again, it was found to be most effective when used at 12.5% w/w, resulting in 7 PF and 5 BF. An increase of PG to 25% w/w led to the identification of 4 PF and 2 BF, while a further increase to 50% resulted in 4 PF and 3 BF. Interestingly, the highest BF/PF ratio (0.75) was observed when the maximum concentration of propylene glycol was used. Based on these observations, PG can be considered as the most promising liquid filler in photopolymer formulations for pharmaceutical SLA 3D printing. Indeed, as it can be loaded at higher concentrations without major effects on printability, and being a smaller molecule (76.1 Da (Zar et al., 2007)) compared to PEG 300, it holds the potential to act as an efficient drug release-enhancer in SLA 3D printed dosage forms.

Surprisingly, glycerol was instead found to be unmixable with PEGDA of any Mn. When added to PEGDA, glycerol caused a distinguishable phase separation of the photopolymer mixture thus resulting in poor printability. Likely, this was caused by the higher hydrophilicity of glycerol due to the presence of 3 hydroxyl groups per molecule. For the purpose of this paper, results of glycerol based formulations are not reported.

3.4.3 N-vinyl pyrrolidone (N-VP)

N-VP was included in our systematic screening as a reactive monomer with the view to improve geometrical accuracy of the 3D printed tablets and to consider its future use as a potential drug release tuning agent. Besides providing higher double bond conversion, N-VP also acts as an oxygen scavenger and is used to improve the photopolymerisation of acrylate-based monomers or macromers (Kim et al., 2019). Here, it was used in combination with PEGDA at a concentration of 5%, 10% and 20% w/w. The use of 5% N-VP allowed identification of 5 PF and 4 BF, with a BF/PF ratio of 0.80 (figure 7). When N-VP concentration was increased to 10% and 20% w/w, printability results worsened showing comparable results.
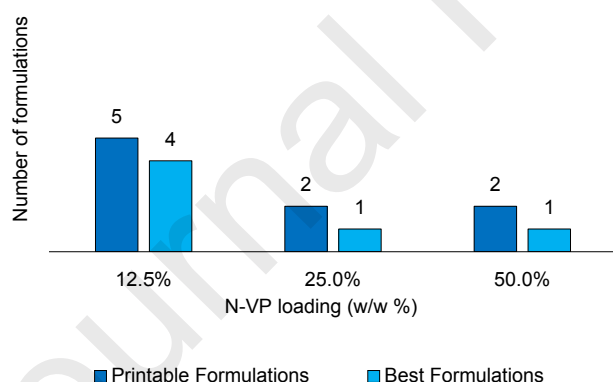
Figure 7. Number of formulations containing N-VP classified as printable formulations (PF) and best formulations (BF).

As expected, the inclusion of N-VP in the photopolymer resins led to higher double bond conversion resulting in hardening of the 3D printed tablets, which became visibly tough and difficult to remove from the build platform. Furthermore, even after 3DP and removal of the uncured resin, 3D printed dosage forms were characterised by a strong N-VP odour, possibly indicating the presence of uncured residues and potentially a toxicity concern. It should be however considered that while N-VP is highly toxic as a monomer, its polymerised form (polyvinylpyrrolidone or PVP), is a commonly used pharmaceutical excipient known to be safe (Ong et al., 2023). Recent research on 3D printed photopolymerised N-VP has shown no tissue damage

in *in-vivo* single-dose acute toxicity studies in rats but of course further investigation is required (Ong et al., 2023).

For this reason, N-VP was not furtherly investigated. However, since it is known that N-VP copolymerises with acrylates and becomes part of the cured matrix (Kim et al., 2019), the interest for its use to generate crosslinked polyvinylpyrrolidone (PVP) in situ through SLA 3DP remains.

3.4.4 Photoinitiator concentration

TPO was used at concentrations of 1%, 0.5%, 0.1%, and 0.05% w/w. As it can be seen in figure 8, the number of formulations classified as PF and BF increases with the decrease of TPO concentration. Indeed, only 7 PF and 4 BF were related to the use of 1% TPO. On the contrary, 0.05% TPO produced 24 PF and 20 BF. This is furtherly evidenced by the high BF/PF ratio related to 0.05% w/w TPO (0.83).

Our results demonstrate that TPO is more effective at low concentrations, providing better printability outcomes. Furthermore, using lower amounts of TPO can bring significant advantages such as reducing any photoinitiator-related toxicity concerns, reducing costs, and potentially increasing drug loading. It is also particularly interesting to note that we found a working TPO concentration 20 times lower than the one generally used for SLA 3D printing of medicines (Robles Martinez et al., 2019; Wang et al., 2016).
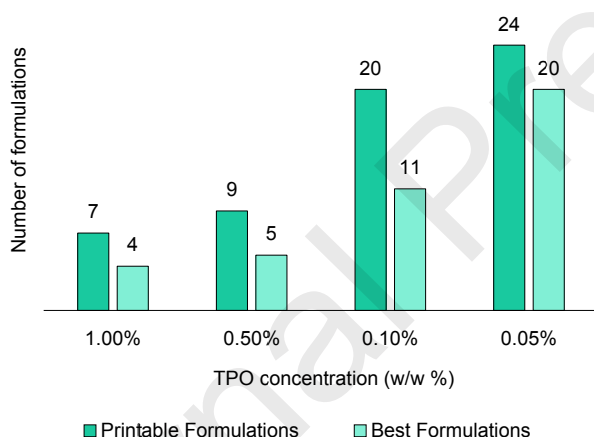
Figure 8. Number of formulations containing TPO in different amounts and classified as printable formulations (PF) and best formulations (BF).

This research describes for the first time the relationship between formulation factors and printability outcomes of 156 photopolymer formulations for pharmaceutical SLA 3D printing, a technique known to be limited in its application due to the narrow choice of available materials. As such, this work has positive implications for the future development of pharmaceutical SLA. Furthermore, in an effort to reduce formulation costs and potentially increase safety and biocompatibility, we found that formulations containing as low as 0.05% w/w TPO not only were printable but also resulted in better printability compared to higher TPO concentrations. This is a dramatic decrease from the commonly used TPO range (0.5% - 1%), allowing for a 10-to-20-fold reduction in the concentration of such photoinitiator.

The overall aim of this work was achieved by identifying suitable PI for SLA 3D printing, followed by the systematic printability screening of 156 photopolymer formulations and the investigation of formulation factors on printability outcomes.

This work provides advantages to pharmaceutical scientists working on SLA 3DP since a large number of photopolymer formulations have been tested, saving time and resources that would otherwise be invested in printability screening. Furthermore, the methodology applied to this research to provide an insight on formulation factors' impact on printability can be similarly applied to other materials to expand the knowledge of SLA biocompatible materials for pharmaceutical applications.

A drawback of this work could be that the screening conducted would necessarily be limited to the printer in use since no standard, pharmaceutical grade SLA 3D printers are currently available. However, most of commercially available SLA 3D printers operates with a 405 nm laser, same as the 3D printer used in this research. It should be considered that among process factors, laser wavelength is the most critical factor for determining the effectiveness of a given PI, based on the PI λ max. Other process factors, such as laser scanning speed or laser power, and responses such as the degree of conversion of printed dosage forms, should be included in future screening aimed to deepen the knowledge on pharmaceutical photopolymerizable formulations.

4. Conclusions

The primary aim of this paper was to provide an insight on the formulation factors to consider in the design and development of photopolymer resins with suitable printability for SLA 3D printing of medicines. First, we identified TPO as the most effective PI in initiating photopolymerisation of PEGDA based photopolymer formulations for SLA 3DP using a 405 nm laser. Then, we have investigated for the first time the influence of several formulation factors on the printability outcomes of 156 photopolymer formulations. Our findings indicate that low molecular weight (Mn 250) PEGDA is an excellent photocrosslinkable polymer although the use of a higher molecular weight (Mn 700) can be recommended due to the greater printability accuracy observed. With regards to the use of liquid fillers as PEG300 and PG, our results suggest that they can be used in low amounts (12.5% w/w) without affecting printability, while caution should be taken in increasing their amount up to 50% w/w due to decrease in printing quality; furthermore, we found that glycerol cannot be mixed in any ratio with PEGDA. Finally, we demonstrated that reducing the amount of photoinitiator (TPO) as low as 0.05% w/w leads to the best printability outcomes as well as introducing advantages such as reduced cost and lower dose-related toxicity concerns.

References

Bail, R., Hong, J.Y., Chin, B.D., 2016. Effect of a red-shifted benzotriazole UV absorber on curing depth and kinetics in visible light initiated photopolymer resins for 3D printing. Journal of Industrial and Engineering Chemistry 38, 141–145. https://doi.org/10.1016/j.jiec.2016.04.017

Bertolotti, S.G., Previtali, C.M., Rufs, A.M., Encinas, M. V, 1999. Riboflavin/triethanolamine as photoinitiator system of vinyl polymerization. A mechanistic study by laser flash photolysis. Macromolecules 32, 2920–2924. https://doi.org/10.1021/ma981246f

Cazin, I., Gleirscher, M.O., Fleisch, M., Berer, M., Sangermano, M., Schlögl, S., 2022. Spatially controlling the mechanical properties of 3D printed objects by dual-wavelength vat photopolymerization. Addit Manuf 57. https://doi.org/10.1016/j.addma.2022.102977

Chen, H., Zhu, D., Kavalli, T., Xiao, P., Schmitt, M., Lalevée, J., 2023. Photopolymerization using bio-sourced photoinitiators. Polym. Chem. 14, 3543–3568. https://doi.org/10.1039/d3py00651d

Chen, Lijuan, Chen, F., Zhu, W., Chen, Luoyi, Liang, Y., Guo, X., 2022. Construction of Photoinitiator Functionalized Spherical Nanoparticles Enabling Favorable Photoinitiating Activity and Migration Resistance for 3D Printing. Polymers (Basel) 14. https://doi.org/10.3390/polym14214551

Commented [CC5]: New reference added.

Chiulan, I., Heggset, E.B., Voicu, Ş.I., Chinga-Carrasco, G., 2021. Photopolymerization of bio-based polymers in a biomedical engineering perspective. Biomacromolecules 22, 1795–1814. https://doi.org/10.1021/acs.biomac.0c01745

Curti, C., Kirby, D.J., Russell, C.A., 2021. Stereolithography apparatus evolution: Enhancing throughput and efficiency of pharmaceutical formulation development. Pharmaceutics 13. https://doi.org/10.3390/pharmaceutics13050616

Curti, C., Kirby, D.J., Russell, C.A., 2020. Current formulation approaches in design and development of solid oral dosage forms through three-dimensional printing. Progress in Additive Manufacturing 5, 111–123. https://doi.org/10.1007/s40964-020-00127-5

Dooms, M., Carvalho, M., 2018. Compounded medication for patients with rare diseases. Orphanet J Rare Dis 13, 1–8. https://doi.org/10.1186/s13023-017-0741-y

Eibel, A., Fast, D.E., Gescheidt, G., 2018. Choosing the ideal photoinitiator for free radical photopolymerizations: Predictions based on simulations using established data. Polym Chem 9, 5107–5115. https://doi.org/10.1039/c8py01195h

Elbadawi, M., Muñiz Castro, B., Gavins, F.K.H., Ong, J.J., Gaisford, S., Pérez, G., Basit, A.W., Cabalar, P., Goyanes, A., 2020. M3DISEEN: A novel machine learning approach for predicting the 3D printability of medicines. Int J Pharm 590, 119837. https://doi.org/10.1016/j.ijpharm.2020.119837

Fouassier, J.P., Allonas, X., Burget, D., 2003. Photopolymerization reactions under visible lights: Principle, mechanisms and examples of applications. Prog Org Coat 47, 16–36. https://doi.org/10.1016/S0300-9440(03)00011-0

Gong, H., Bickham, B.P., Woolley, A.T., Nordin, G.P., 2017. Custom 3D printer and resin for 18 μm × 20 μm microfluidic flow channels. Lab Chip 17, 2899–2909. https://doi.org/10.1039/c7lc00644f

Goyanes, A., Madla, C.M., Umerji, A., Duran Piñeiro, G., Giraldez Montero, J.M., Lamas Diaz, M.J., Gonzalez Barcia, M., Taherali, F., Sánchez-Pintos, P., Couce, M.L., Gaisford, S., Basit, A.W., 2019. Automated therapy preparation of isoleucine formulations using 3D printing for the treatment of MSUD: First single-centre, prospective, crossover study in patients. Int J Pharm 567, 118497. https://doi.org/10.1016/j.ijpharm.2019.118497

Jeencham, R., Tawonsawatruk, T., Numpaisal, P.O., Ruksakulpiwat, Y., 2023. Reinforcement of Injectable Hydrogel for Meniscus Tissue Engineering by Using Cellulose Nanofiber from Cassava Pulp. Polymers (Basel). 15. https://doi.org/10.3390/polym15092092

Kamoun, E.A., Winkel, A., Eisenburger, M., Menzel, H., 2016. Carboxylated camphorquinone as visible-light photoinitiator for biomedical application: Synthesis, characterization, and application Carboxylated camphorquinone as visible-light photoinitiator. Arabian Journal of Chemistry 9, 745–754. https://doi.org/10.1016/j.arabjc.2014.03.008

Karavasili, C., Gkaragkounis, A., Moschakis, T., Ritzoulis, C., Fatouros, D.G., 2020. Pediatric-friendly chocolate-based dosage forms for the oral administration of both hydrophilic and lipophilic drugs fabricated with extrusion-based 3D printing. European Journal of Pharmaceutical Sciences 147, 105291. https://doi.org/10.1016/j.ejps.2020.105291

Khaled, S.A., Alexander, M.R., Wildman, R.D., Wallace, M.J., Sharpe, S., Yoo, J., Roberts, C.J., 2018. 3D extrusion printing of high drug loading immediate release paracetamol tablets. Int J Pharm 538, 223–230. https://doi.org/10.1016/j.ijpharm.2018.01.024

Khaled, S.A., Burley, J.C., Alexander, M.R., Yang, J., Roberts, C.J., 2015. 3D printing of tablets containing multiple drugs with defined release profiles. Int J Pharm 494, 643–650. https://doi.org/10.1016/j.ijpharm.2015.07.067

Commented [CC6]: New reference added.

Commented [CC7]: New reference added.

Kim, D.S. (Danny), Suriboot, J., Grunlan, M.A., Tai, B.L., 2019. Feasibility study of silicone stereolithography with an optically created dead zone. Addit Manuf 29, 100793. https://doi.org/10.1016/j.addma.2019.100793

Kochhar, J.S., Zou, S., Chan, S.Y., Kang, L., 2012. Protein encapsulation in polymeric microneedles by photolithography. Int J Nanomedicine 7, 3143–3154. https://doi.org/10.2147/IJN.S32000

Konasch, J., Riess, A., Teske, M., Rekowska, N., Mau, R., Eickner, T., Grabow, N., Seitz, H., 2018. Novel 3D printing concept for the fabrication of time-controlled drug delivery systems. Current Directions in Biomedical Engineering 4, 141–144. https://doi.org/10.1515/cdbme-2018-0035

Konta, A., García-Piña, M., Serrano, D., 2017. Personalised 3D Printed Medicines: Which Techniques and Polymers Are More Successful? Bioengineering 4, 79. https://doi.org/10.3390/bioengineering4040079

Krkobabić, M., Medarević, D., Cvijić, S., Grujić, B., Ibrić, S., 2019. Hydrophilic excipients in digital light processing (DLP) printing of sustained release tablets: Impact on internal structure and drug dissolution rate. Int J Pharm 572, 118790. https://doi.org/10.1016/j.ijpharm.2019.118790

Lakkala, P., Munnangi, S.R., Bandari, S., Repka, M., 2023. Additive manufacturing technologies with emphasis on stereolithography 3D printing in pharmaceutical and medical applications: A review. Int J Pharm X 5, 100159. https://doi.org/10.1016/j.ijpx.2023.100159

Li, N., Khan, S.B., Chen, S., Aiyiti, W., Zhou, J., Lu, B., 2023. Promising New Horizons in Medicine: Medical Advancements with Nanocomposite Manufacturing via 3D Printing. Polymers (Basel). 15. https://doi.org/10.3390/polym15204122

Li, Q., Guan, X., Cui, M., Zhu, Z., Chen, K., Wen, H., Jia, D., Hou, J., Xu, W., Yang, X., Pan, W., 2018. Preparation and investigation of novel gastro-floating tablets with 3D extrusion-based printing. Int J Pharm 535, 325–332. https://doi.org/10.1016/j.ijpharm.2017.10.037

Martinez, P.R., Goyanes, A., Basit, A.W., Gaisford, S., 2017. Fabrication of drug-loaded hydrogels with stereolithographic 3D printing. Int J Pharm 532, 313–317. https://doi.org/10.1016/j.ijpharm.2017.09.003

Meereis, C.T.W., Leal, F.B., Lima, G.S., De Carvalho, R. V, Piva, E., Ogliari, F.A., 2014. BAPO as an alternative photoinitiator for the radical polymerization of dental resins. Dental Materials 30, 945–953. https://doi.org/10.1016/j.dental.2014.05.020

Muhindo, D., Elkanayati, R., Srinivasan, P., Repka, M.A., Ashour, E.A., 2023. Recent Advances in the Applications of Additive Manufacturing (3D Printing) in Drug Delivery: A Comprehensive Review. AAPS PharmSciTech 24, 1–22. https://doi.org/10.1208/s12249-023-02524-9

Nan, X., Sun, L., Luo, Y., Wu, M., Chen, G., 2022. Glycine derivatives with closed carboxyl group as effective co-initiators for radical photopolymerization in the presence of camphorquinone. Polymer Bulletin 79, 10865–10880. https://doi.org/10.1007/s00289-022-04074-9

Ong, J.J., Chow, Y.L., Gaisford, S., Cook, M.T., Swift, T., Telford, R., Rimmer, S., Qin, Y., Mai, Y., Goyanes, A., Basit, A.W., 2023. Supramolecular chemistry enables vat photopolymerization 3D printing of novel water-soluble tablets. Int J Pharm 643, 123286. https://doi.org/10.1016/j.ijpharm.2023.123286

Pan, S., Ding, S., Zhou, X., Zheng, N., Zheng, M., Wang, J., Yang, Q., Yang, G., 2023. 3D-printed dosage forms for oral administration: a review. Drug Deliv. Transl. Res. https://doi.org/10.1007/s13346-023-01414-8

Commented [CC8]: New reference added.

Commented [CC9]: New reference added.

Commented [CC10]: New reference added.

Patel, K.R., Prajapati, L.M., Joshi, A.K., Kharodiya, M.L., Patel, J.R., 2013. Application of chemometrics in simultaneous spectrophotometric quantification of etophylline and theophylline: The drugs with same chromophore. Iranian Journal of Pharmaceutical Sciences 9, 17–28.

Pan, W., Wallin, T.J., Odent, J., Yip, M.C., Mosadegh, B., Shepherd, R.F., Giannelis, E.P., 2019. Optical stereolithography of antifouling zwitterionic hydrogels. J. Mater. Chem. B 7, 2855–2864. https://doi.org/10.1039/c9tb00278b

Pariskar, A., Sharma, P.K., Murty, U.S., Banerjee, S., 2023. Effect of Tartrazine as Photoabsorber for Improved Printing Resolution of 3D Printed "Ghost Tablets": Non-Erodible Inert Matrices. J. Pharm. Sci. 112, 1020–1031. https://doi.org/10.1016/j.xphs.2022.11.014

Pietrzak, K., Isreb, A., Alhnan, M.A., 2015. A flexible-dose dispenser for immediate and extended release 3D printed tablets. European Journal of Pharmaceutics and Biopharmaceutics 96, 380–387. https://doi.org/10.1016/j.ejpb.2015.07.027

Robles Martinez, P., Basit, A.W., Gaisford, S., 2018. The history, developments and opportunities of stereolithography. AAPS Advances in the Pharmaceutical Sciences Series 31, 55–79. https://doi.org/10.1007/978-3-319-90755-0_4

Robles Martinez, P., Xu, X., Trenfield, S.J., Awad, A., Goyanes, A., Telford, R., Basit, A.W., Gaisford, S., 2019. 3D Printing of a Multi-Layered Polypill Containing Six Drugs Using a Novel Stereolithographic Method.

Rossegger, E., Shaukat, U., Moazzen, K., Fleisch, M., Berer, M., Schlögl, S., 2023a. The effect of photolatent catalysts on the exchange kinetics of dual-wavelength 3D printable and photopatternable thiol-click vitrimers. Polym Chem 14, 2640–2651. https://doi.org/10.1039/d3py00333g

Rossegger, E., Strasser, J., Höller, R., Fleisch, M., Berer, M., Schlögl, S., 2023b. Wavelength Selective Multi-Material 3D Printing of Soft Active Devices Using Orthogonal Photoreactions. Macromol Rapid Commun 44, 1–9. https://doi.org/10.1002/marc.202200586

Seoane-Viaño, I., Trenfield, S.J., Basit, A.W., Goyanes, A., 2021. Translating 3D printed pharmaceuticals: From hype to real-world clinical applications. Adv Drug Deliv Rev 174, 553–575. https://doi.org/10.1016/j.addr.2021.05.003

Seoane-Viaño, I., Ong, J.J., Basit, A.W., Goyanes, A., 2022. To infinity and beyond: Strategies for fabricating medicines in outer space. Int. J. Pharm. X 4, 29–39. https://doi.org/10.1016/j.ijpx.2022.100121

Serrano, D.R., Kara, A., Yuste, I., Luciano, F.C., Ongoren, B., Anaya, B.J., Molina, G., Diez, L., Ramirez, B.I., Ramirez, I.O., Sánchez-Guirales, S.A., Fernández-García, R., Bautista, L., Ruiz, H.K., Lalatsa, A., 2023. 3D Printing Technologies in Personalized Medicine, Nanomedicines, and Biopharmaceuticals. Pharmaceutics 15. https://doi.org/10.3390/pharmaceutics15020313

Sirajuddin, Khaskheli, A.R., Shah, A., Bhanger, M.I., Niaz, A., Mahesar, S., 2007. Simpler spectrophotometric assay of paracetamol in tablets and urine samples. Spectrochim Acta A Mol Biomol Spectrosc 68, 747–751. https://doi.org/10.1016/j.saa.2006.12.055

Tagami, T., Ito, E., Kida, R., Hirose, K., Noda, T., Ozeki, T., 2021. 3D printing of gummy drug formulations composed of gelatin and an HPMC-based hydrogel for pediatric use. Int J Pharm 594, 120118. https://doi.org/10.1016/j.ijpharm.2020.120118

Trenfield, S.J., Xu, X., Goyanes, A., Rowland, M., Wilsdon, D., Gaisford, S., Basit, A.W., 2023. Releasing fast and slow: Non-destructive prediction of density and drug release from SLS 3D printed tablets using NIR spectroscopy. Int J Pharm X 5, 100148. https://doi.org/10.1016/j.ijpx.2022.100148

Commented [CC11]: New reference added.

Commented [CC12]: New reference added.

Van Der Linden, P.J.E.M., Popov, A.M., Pontoni, D., 2020. Accurate and rapid 3D printing of microfluidic devices using wavelength selection on a DLP printer. Lab Chip 20, 4128–4140. https://doi.org/10.1039/d0lc00767f

Voet, V.S.D., Strating, T., Schnelting, G.H.M., Dijkstra, P., Tietema, M., Xu, J., Woortman, A.J.J., Loos, K., Jager, J., Folkersma, R., 2018. Biobased Acrylate Photocurable Resin Formulation for Stereolithography 3D Printing. ACS Omega 3, 1403–1408. https://doi.org/10.1021/acsomega.7b01648

Wang, J., Goyanes, A., Gaisford, S., Basit, A.W., 2016. Stereolithographic (SLA) 3D printing of oral modified-release dosage forms. Int J Pharm 503, 207–212. https://doi.org/10.1016/j.ijpharm.2016.03.016

Williams, C.G., Malik, A.N., Kim, T.K., Manson, P.N., Elisseeff, J.H., 2005. Variable cytocompatibility of six cell lines with photoinitiators used for polymerizing hydrogels and cell encapsulation. Biomaterials 26, 1211–1218. https://doi.org/10.1016/j.biomaterials.2004.04.024

Xu, X., Awad, A., Robles Martinez, P., Gaisford, S., Goyanes, A., Basit, A.W., 2021. Vat photopolymerization 3D printing for advanced drug delivery and medical device applications. Journal of Controlled Release 329, 743–757. https://doi.org/10.1016/j.jconrel.2020.10.008

Xu, X., Robles Martinez, P., Madla, C.M., Joubert, F., Goyanes, A., Basit, A.W., Gaisford, S., 2020. Stereolithography (SLA) 3D printing of an antihypertensive polyprintlet: Case study of an unexpected photopolymer-drug reaction. Addit Manuf 33, 101071. https://doi.org/10.1016/j.addma.2020.101071

Zakeri, S., Vippola, M., Levänen, E., 2020. A comprehensive review of the photopolymerization of ceramic resins used in stereolithography. Addit Manuf 35, 101177. https://doi.org/10.1016/j.addma.2020.101177

Zanon, M., Baruffaldi, D., Sangermano, M., Pirri, C.F., Frascella, F., Chiappone, A., 2021. Visible light-induced crosslinking of unmodified gelatin with PEGDA for DLP-3D printable hydrogels. Eur Polym J 160. https://doi.org/10.1016/j.eurpolymj.2021.110813

Zar, T., Graeber, C., Perazella, M.A., 2007. Recognition, treatment, and prevention of propylene glycol toxicity. Semin Dial 20, 217–219. https://doi.org/10.1111/j.1525-139X.2007.00280.x

Table A.1. % w/w composition of the 156 photopolymer formulations prepared and screened. The classification group assigned after printing is also reported.

	PEGDA 250	PEGDA 575	PEGDA 700	PEG 300	Propylene Glycol	Glycerol	N-Vynil Pyrrolidone	TPO	Group assigned
F1	99.00	-	-	-	-	-	-	1.00	B1
F2	99.50	-	-	-	-	-	-	0.50	B1

F3	99.90	-	-	-	-	-	-	0.10	B1
F4	99.95	-	-	-	-	-	-	0.05	A
F5	-	99.00	-	-	-	-	-	1.00	A
F6	-	99.50	-	-	-	-	-	0.50	A
F7	-	99.90	-	-	-	-	-	0.10	B1
F8	-	99.95	-	-	-	-	-	0.05	A
F9	-	-	99.00	-	-	-	-	1.00	A
F10	-	-	99.50	-	-	-	-	0.50	A
F11	-	-	99.90	-	-	-	-	0.10	B1
F12	-	-	99.95	-	-	-	-	0.05	B1
F13	86.50	-	-	12.50	-	-	-	1.00	B1
F14	74.00	-	-	25.00	-	-	-	1.00	A
F15	49.00	-	-	50.00	-	-	-	1.00	A
F16	87.00	-	-	12.50	-	-	-	0.50	A
F17	74.50	-	-	25.00	-	-	-	0.50	A
F18	49.50	-	-	50.00	-	-	-	0.50	A
F19	87.40	-	-	12.50	-	-	-	0.10	B1
F20	74.90	-	-	25.00	-	-	-	0.10	A
F21	49.90	-	-	50.00	-	-	-	0.10	A
F22	87.45	-	-	12.50	-	-	-	0.05	A

F23	74.95	-	-	25.00	-	-	-	0.05	B
F24	49.95	-	-	50.00	-	-	-	0.05	A
F25	-	86.50	-	12.50	-	-	-	1.00	B
F26	-	74.00	-	25.00	-	-	-	1.00	A
F27	-	49.00	-	50.00	-	-	-	1.00	A
F28	-	87.00	-	12.50	-	-	-	0.50	A
F29	-	74.50	-	25.00	-	-	-	0.50	B
F30	-	49.50	-	50.00	-	-	-	0.50	A
F31	-	87.40	-	12.50	-	-	-	0.10	B
F32	-	74.90	-	25.00	-	-	-	0.10	A
F33	-	49.90	-	50.00	-	-	-	0.10	A
F34	-	87.45	-	12.50	-	-	-	0.05	B1
F35	-	74.95	-	25.00	-	-	-	0.05	B1
F36	-	49.95	-	50.00	-	-	-	0.05	A
F37	-	-	86.50	12.50	-	-	-	1.00	A
F38	-	-	74.00	25.00	-	-	-	1.00	A
F39	-	-	49.00	50.00	-	-	-	1.00	A
F40	-	-	87.00	12.50	-	-	-	0.50	A
F41	-	-	74.50	25.00	-	-	-	0.50	A
F42	-	-	49.50	50.00	-	-	-	0.50	A

F43	-	-	87.40	12.50	-	-	-	0.10	A
F44	-	-	74.90	25.00	-	-	-	0.10	A
F45	-	-	49.90	50.00	-	-	-	0.10	A
F46	-	-	87.45	12.50	-	-	-	0.05	B2
F47	-	-	74.95	25.00	-	-	-	0.05	A
F48	-	-	49.95	50.00	-	-	-	0.05	A
F49	-	86.50	-	-	12.50	-	-	1.00	A
F50	-	74.00	-	-	25.00	-	-	1.00	A
F51	-	49.00	-	-	50.00	-	-	1.00	A
F52	-	87.00	-	-	12.50	-	-	0.50	A
F53	-	74.50	-	-	25.00	-	-	0.50	A
F54	-	49.50	-	-	50.00	-	-	0.50	A
F55	-	87.40	-	-	12.50	-	-	0.10	B
F56	-	74.90	-	-	25.00	-	-	0.10	B
F57	-	49.90	-	-	50.00	-	-	0.10	B
F58	-	87.45	-	-	12.50	-	-	0.05	B1
F59	-	74.95	-	-	25.00	-	-	0.05	B1
F60	-	49.95	-	-	50.00	-	-	0.05	B1
F61	-	-	86.50	-	12.50	-	-	1.00	A
F62	-	-	74.00	-	25.00	-	-	1.00	A

F63	-	-	49.00	-	50.00	-	-	1.00	A
F64	-	-	87.00	-	12.50	-	-	0.50	A
F65	-	-	74.50	-	25.00	-	-	0.50	A
F66	-	-	49.50	-	50.00	-	-	0.50	A
F67	-	-	87.40	-	12.50	-	-	0.10	B
F68	-	-	74.90	-	25.00	-	-	0.10	A
F69	-	-	49.90	-	50.00	-	-	0.10	A
F70	-	-	87.45	-	12.50	-	-	0.05	B2
F71	-	-	74.95	-	25.00	-	-	0.05	B1
F72	-	-	49.95	-	50.00	-	-	0.05	B1
F73	-	86.50	-	-	-	12.50	-	1.00	A
F74	-	74.00	-	-	-	25.00	-	1.00	A
F75	-	49.00	-	-	-	50.00	-	1.00	A
F76	-	87.00	-	-	-	12.50	-	0.50	B
F77	-	74.50	-	-	-	25.00	-	0.50	A
F78	-	49.50	-	-	-	50.00	-	0.50	A
F79	-	87.40	-	-	-	12.50	-	0.10	B1
F80	-	74.90	-	-	-	25.00	-	0.10	B
F81	-	49.90	-	-	-	50.00	-	0.10	B
F82	-	87.45	-	-	-	12.50	-	0.05	B1

F83	-	74.95	-	-	-	25.00	-	0.05	B1
F84	-	49.95	-	-	-	50.00	-	0.05	B2
F85	-	-	86.50	-	-	12.50	-	1.00	A
F86	-	-	74.00	-	-	25.00	-	1.00	A
F87	-	-	49.00	-	-	50.00	-	1.00	A
F88	-	-	87.00	-	-	12.50	-	0.50	A
F89	-	-	74.50	-	-	25.00	-	0.50	A
F90	-	-	49.50	-	-	50.00	-	0.50	A
F91	-	-	87.40	-	-	12.50	-	0.10	B
F92	-	-	74.90	-	-	25.00	-	0.10	A
F93	-	-	49.90	-	-	50.00	-	0.10	A
F94	-	-	87.45	-	-	12.50	-	0.05	B1
F95	-	-	74.95	-	-	25.00	-	0.05	B1
F96	-	-	49.95	-	-	50.00	-	0.05	A
F97	-	-	94.00	-	-	-	5.00	1.00	A
F98	-	-	89.00	-	-	-	10.00	1.00	A
F99	-	-	79.00	-	-	-	20.00	1.00	A
F100	-	-	94.50	-	-	-	5.00	0.50	A
F101	-	-	89.50	-	-	-	10.00	0.50	A
F102	-	-	79.50	-	-	-	20.00	0.50	A

F103	-	-	94.90	-	-	-	5.00	0.10	A
F104	-	-	89.90	-	-	-	10.00	0.10	A
F105	-	-	79.90	-	-	-	20.00	0.10	A
F106	-	-	94.95	-	-	-	5.00	0.05	A
F107	-	-	89.95	-	-	-	10.00	0.05	A
F108	-	-	79.95	-	-	-	20.00	0.05	A
F109	-	94.00	-	-	-	-	5.00	1.00	A
F110	-	89.00	-	-	-	-	10.00	1.00	A
F111	-	79.00	-	-	-	-	20.00	1.00	A
F112	-	94.50	-	-	-	-	5.00	0.50	A
F113	-	89.50	-	-	-	-	10.00	0.50	A
F114	-	79.50	-	-	-	-	20.00	0.50	B
F115	-	94.90	-	-	-	-	5.00	0.10	B1
F116	-	89.90	-	-	-	-	10.00	0.10	A
F117	-	79.90	-	-	-	-	20.00	0.10	A
F118	-	94.95	-	-	-	-	5.00	0.05	B1
F119	-	89.95	-	-	-	-	10.00	0.05	B
F120	-	79.95	-	-	-	-	20.00	0.05	B1
F121	94.00	-	-	-	-	-	5.00	1.00	A
F122	89.00	-	-	-	-	-	10.00	1.00	A

Journal Pre-proofs

F123	79.00	-	-	-	-	-	20.00	1.00	A
F124	94.50	-	-	-	-	-	5.00	0.50	B
F125	89.50	-	-	-	-	-	10.00	0.50	A
F126	79.50	-	-	-	-	-	20.00	0.50	A
F127	94.90	-	-	-	-	-	5.00	0.10	B1
F128	89.90	-	-	-	-	-	10.00	0.10	A
F129	79.90	-	-	-	-	-	20.00	0.10	A
F130	94.95	-	-	-	-	-	5.00	0.05	B1
F131	89.95	-	-	-	-	-	10.00	0.05	B1
F132	79.95	-	-	-	-	-	20.00	0.05	A
F133	86.50	-	-	-	-	12.50	-	1.00	B1
F134	74.00	-	-	-	-	25.00	-	1.00	B
F135	49.00	-	-	-	-	50.00	-	1.00	B
F136	87.00	-	-	-	-	12.50	-	0.50	B2
F137	74.50	-	-	-	-	25.00	-	0.50	B1
F138	49.50	-	-	-	-	50.00	-	0.50	B1
F139	87.40	-	-	-	-	12.50	-	0.10	B2
F140	74.90	-	-	-	-	25.00	-	0.10	B1
F141	49.90	-	-	-	-	50.00	-	0.10	B1
F142	87.45	-	-	-	-	12.50	-	0.05	A

F143	74.95	-	-	-	-	25.00	-	0.05	B
F144	49.95	-	-	-	-	50.00	-	0.05	B
F145	86.50	-	-	-	12.50	-	-	1.00	B1
F146	74.00	-	-	-	25.00	-	-	1.00	A
F147	49.00	-	-	-	50.00	-	-	1.00	A
F148	87.00	-	-	-	12.50	-	-	0.50	B1
F149	74.50	-	-	-	25.00	-	-	0.50	A
F150	49.50	-	-	-	50.00	-	-	0.50	A
F151	87.40	-	-	-	12.50	-	-	0.10	B1
F152	74.90	-	-	-	25.00	-	-	0.10	B
F153	49.90	-	-	-	50.00	-	-	0.10	A
F154	87.45	-	-	-	12.50	-	-	0.05	A
F155	74.95	-	-	-	25.00	-	-	0.05	A
F156	49.95	-	-	-	50.00	-	-	0.05	B1

Author Contributions

Carlo Curti – CC

Daniel Kirby – DK

Craig Russell – CR

Conceptualization – CC, DK, CR

Data curation – CC, CR

Formal analysis – CC, CR

Funding acquisition – DK, CR

Investigation – CC, DK, CR

Methodology – CC, DK, CR

Project administration – DK, CR

Resources – CC, DK, CR

Software – CC, DK, CR

Supervision – DK, CR

Validation – CC, CR

Visualization – CC, DK, CR

Roles/Writing - original draft – CC

Writing - review & editing – CC, DK, CR

Declaration of interests

☒ The authors declare that they have no known competing financial interests or personal relationships that could have appeared to influence the work reported in this paper.

☐ The authors declare the following financial interests/personal relationships which may be considered as potential competing interests:
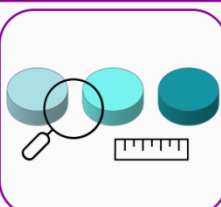
Systematic screening of photopolymer resins for Stereolithography (SLA) 3D printing of solid oral dosage forms: investigation of formulation factors on printability outcomes.
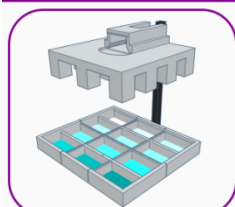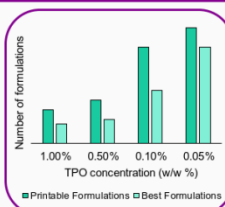
I. Design and preparation of 156 photopolymer formulations
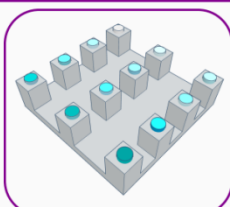
II. Stereolithography 3D printing of tablets using a modified SLA apparatus

III. Visual observation of 3D printed tablets and printability score assignation

IV. Evaluation of formulations factors on printability outcomes

CONCLUSION
- Reducing the amount of photoinitiator improves printability outcomes
- Large amounts of PEG300 and propylene glycol as liquid fillers can decrease printing quality
- Glycerol is immiscible with PEGDA hence cannot be used as a liquid filler

Aston University
BIRMINGHAM UK

Visual abstract by Carlo Curti, PhD